



# Set-up for an Optically Induced Dielectrophoresis Platform and Its Use in Manipulating Micro- and Nanoscale Materials

Yen-Heng Lin<sup>1,2,\*</sup>, Kai-Siang Ho<sup>1</sup>, and Chin-Tien Yang<sup>3</sup>

<sup>1</sup>Department of Electronic Engineering, Chang Gung University, Taoyuan 333, Taiwan

<sup>2</sup>Graduate Institute of Medical Mechatronics, Chang Gung University, Taoyuan 333, Taiwan

<sup>3</sup>Material and Chemical Research Laboratories, Industrial Technology Research Institute, Hsinchu, Taiwan

(Received 30 June 2014; Accepted 12 September 2014; Published on line 1 December 2014)

\*Email: [yenheng@mail.cgu.edu.tw](mailto:yenheng@mail.cgu.edu.tw)

DOI: [10.5875/ausmt.v4i4.797](https://doi.org/10.5875/ausmt.v4i4.797)

**Abstract:** An optically-induced dielectrophoresis platform is proposed to manipulate micro- and nanoscale particles. A commercially available liquid-crystal-display-based projector was used as a light source to produce a variety of optical patterns and project them onto a photoconductive material. The optical patterns illuminating the photoconductive material can be used as configurable virtual electrodes, which will induce dielectrophoretic forces on the particles which can thus be manipulated by dynamic optical patterns. The manipulation of silver nanowires was demonstrated by forming a specific pattern of nanowires through illumination of the photoconductive chip with an optical pattern. Polystyrene beads with diameters of 10 and 20  $\mu\text{m}$  were also successfully manipulated. By combining the optically-induced dielectrophoretic force and the hydrodynamic force, particles of two different sizes can be continuously separated into two different microchannels. Furthermore, the microparticles were collected and concentrated by virtual electrode traps. We believe that this flexible platform can be applied to a variety of fields such as single cell study, nanotechnology, or surface-enhanced Raman spectroscopy.

**Keywords:** Optically induced dielectrophoresis; nanowires; microparticle manipulation; optoelectronic tweezers

## Introduction

The development of fluid-based micro-device technologies have allowed for the miniaturization of systems for biomedical and chemical analysis [1], enabling the manipulation of nanoliter and microliter amounts of fluids. For example, micromixers, micropumps, and microvalves have been developed to transport, mix, and manipulate fluids in a palm-sized apparatus with a microfluidic chip that employs several driving forces including the electromagnetic force, the piezoelectric force, the electrokinetic force, gravity, the

pneumatic force, and the electrostatic force [2-4]. Most of these forces can be used to drive bulk fluids in the microfluidic chip. In contrast with these driving forces that drive the bulk fluid, dielectrophoresis (DEP) can control substances suspended in the fluid, as was first proposed in 1951 [5]. The DEP force is commonly used for the manipulation of dielectric particles, such as biological cells and micro- and nanoparticles. An AC electric field will induce a dipole moment in a dielectric particle suspended in a solution. The dipole moment interacts with the applied ac electric field, generating an attractive DEP force or a repulsive DEP force. The direction of the force depends on the relative



polarizabilities of the particles and the surrounding solution. The magnitude of the DEP force depends on the permittivity and conductivity of both the particle and the medium, as well as the size of the particles. To create a particular DEP force, a specific microelectrode pattern is required to provide the ac electric field in a microfluidic chip. A delicate fabrication process is required to create metal electrodes on the microfluidic chip substrate, entailing tedious fabrication processes are needed to redesign and fabricate patterns for various geometric electrodes. This may limit the degree of manipulation flexibility that can be achieved in applications.

As an alternative approach, optically-induced dielectrophoresis (ODEP) or optoelectronic tweezers (OET) technology using optical images to define configurable virtual electrodes in a microfluidic chip has attracted considerable interest as a way to manipulate micro- and nanoparticles. This technique was first demonstrated by Chiou et al. in 2005 [6]. The OET platform fuses the fields of optoelectronics and biomedicine to provide a highly flexible platform for manipulating cells and nanoparticles. The ODEP technique uses a commercially available projector [7], laser [8], or liquid crystal display (LCD) panel [9] as the light source and uses a photoconductive material as the OET chip substrate. Illuminating the surface of a photoconductive material (usually amorphous silicon) with a light pattern creates a non-uniform electric field and generates dielectrophoretic forces. The optical images serve as a switch and can be used to define virtual electrodes, and thus the OET platform can provide a flexible DEP pattern. The layouts of the driving electrodes are configurable, which is convenient for the manipulation of micro- and nanoparticles. In addition, this approach requires an optical intensity that is 100,000 times less than that required by optical tweezers [6] and provides a high resolution for microparticle manipulation.

The OET platform is a convenient tool for cell studies including cell separation [10], cell electroporation [11], cell lysis [12], and single-cell investigations [13]. For example, the platform allows for the differentiation of different dielectric properties of the cell membrane. By using a moving line image and varying its velocity, rare circulating tumor cells (CTCs) and the leukocyte background can be separated because of the difference in drag forces induced by a positive ODEP force [14]. Scanning line patterns with a positive ODEP force are sufficient for dragging the CTCs, whereas the leukocyte experienced a small ODEP force and thus could not be moved by scanning line patterns with the same scanning velocity. In addition, microfluidic components such as micropumps, microvalves, or micromixers made with

polydimethylsiloxane (PDMS) materials have been integrated with the OET platform [13]. The integrated platform has been used to administer a single-cell-level pretreatment, followed by a quantitative reverse transcription polymerase chain reaction to analyze the interior of the cell.

Furthermore, electroporation can also be performed with the OET platform. Traditional electroporation using electroporation cuvettes cannot deliver genes into a specific cell within a group of cells. The OET platform can selectively perform electroporation through the optically addressable electric field. With multi-triangle optical patterns [11], a high-efficiency transfection can be performed under the OET platform with a higher induced electric field. If the transmembrane potential induced by the external electric field is higher than about 1 V, the pole of the cell membrane becomes irreversibly opened, thus causing cell lysis. Hence, a selective cell lysis can also be achieved by the OET platform [12].

In addition, the OET platform has strong potential for the manipulation of micro- or nanoscale particles. It has been demonstrated that the OET platform can be combined with a surface-enhanced Raman scattering (SERS) detection scheme [8]. Using the OET platform, gold nanoparticles can be manipulated and aggregated at a specific position by shining a laser spot on the photoconductive layer. The SERS signal can then also be excited by the same laser source. The concentration of gold nanoparticles enhances the SERS signal, and thus the detection limit can be further improved by the integrated platform. In addition, other modes of manipulation of microparticles have been demonstrated using the OET platform. For example, our research group has demonstrated optically-induced flow cytometry [15] which can focus, count, and sort microparticles using optical images. Moreover, the magnitude of the generated ODEP force was found to depend on the color, intensity, and physical line width of the illuminating light; these optical properties can be used to allow the OET platform to separate microparticles [16].

In this study, we focus on the set-up of the OET platform, including the light source component, the magnifying mechanism component, and the photoconductive OET chip. One can tailor the system to a given application by selecting an appropriate light source and magnifying mechanism. In addition, the alignment of the optical path is also important for the generation of a clear optical pattern. We also demonstrate the ability of the OET platform to manipulate micro- and nanoparticles. We believe that the versatility of the OET platform makes it suitable for use in a range of applications in biomedical research.



## Materials and methods

### Operation principle of the OET platform

As shown in Fig. 1, the OET chip is formed from a top layer that consists of an indium tin oxide (ITO) glass substrate and a bottom layer that is photoconductive. The photoconductive layer is composed of a thin metal layer and amorphous silicon on top of a piece of ITO glass. An electric dipole moment is induced in particles such as nanowires, cells, or polystyrene beads within the OET chip through the external ac electric field that is applied between the chip's top and bottom layers. Before the photoconductive layer of the OET chip is illuminated, a uniform electric field is generated between the top and bottom layers. Illumination generates electron-hole pairs, decreasing the impedance of the photoconductive layer. Therefore, the electric field, which initially exhibited a uniform strength and orthogonal to the top and bottom layers, becomes a non-uniform electric field. An optically induced effect allows the generation of a virtual electrode on the photoconductive layer. When the particles with induced dipole moments experience the non-uniform electric field, the ODEP force is generated to attract or repel the particles toward or away from the virtual electrodes. This force can be expressed as [17]

$$F_{DEP} = 2\pi r^3 \epsilon_m \text{Re}(f_{CM}) \nabla E^2 \quad (1)$$

where  $r$  is the radius of the particle,  $\epsilon_m$  is the permittivity of the media surrounding the particle,  $E$  is the root-mean-square value of the local electric field, and  $\text{Re}(f_{CM})$  is the real part of the Clausius-Mossotti factor, which can be expressed as

$$f_{CM}(\omega) = \frac{\epsilon_p^* - \epsilon_m^*}{\epsilon_p^* + 2\epsilon_m^*} \quad (2)$$

where  $\epsilon_p^*$  and  $\epsilon_m^*$  are the complex permittivity of the particles and the surrounding medium, respectively. The complex permittivity can be expressed as

$$\epsilon^* = \epsilon - j(\sigma / \omega) \quad (3)$$

This formula shows that the magnitude of the complex permittivity is related to the permittivity ( $\epsilon$ ), the conductance ( $\sigma$ ), and the frequency of the ac electric field driving the particle manipulation ( $\omega$ ). Regulating the frequency of the electric field allows for the tuning of the permittivity, the conductivity of the working medium, and the magnitude and direction (that is, whether the force is attractive or repulsive) of the ODEP force produced in the OET platform.

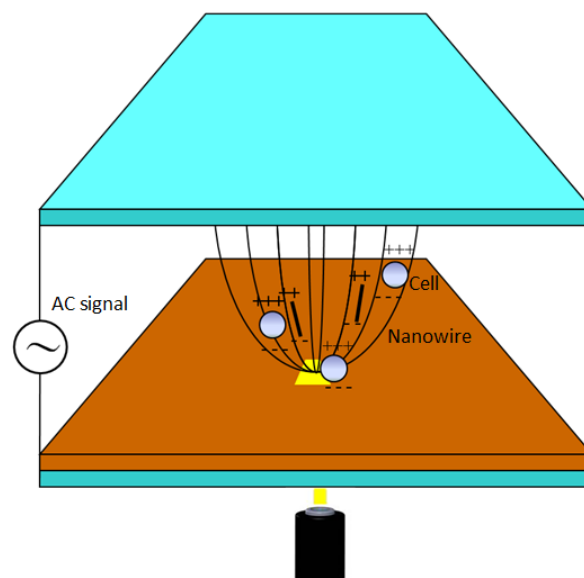


Figure 1. Schematic illustrating the operation principle of ODEP force generation.

### Set-up of the OET platform

Figure 2 shows a schematic illustration of the set-up of the OET platform. It comprises five major parts including the light source, light modulator, OET chip, optical lens, and observation system. The light source and light control unit are used to provide a configurable light pattern that illuminates the OET chip. Several light sources can be used to excite electron-hole pairs in the photoconductive layer, such as a laser, a light-emitting diode (LED), a halogen lamp, or a mercury-vapor lamp. A laser light source has the advantages of a high light/dark contrast ratio and eliminates the need for focusing. However, the laser should be used with a precision x-y

**Yen-Heng Lin** received his M.S. and Ph.D. degrees in Department of Engineering Science from National Cheng Kung University, Taiwan in 2002 and 2009, respectively. He is currently an Assistant Professor (From 2010) in Chang Gung University, Taiwan. His research interests are focused on bio-MEMS, microfluidics, optically-induced dielectrophoresis and its bio-medical applications.

**Kai-Siang Ho** received his B.S. and M.S. degrees in Department of Electronic Engineering from Chang Gung University, Taiwan in 2010 and 2013, respectively. He is currently an Engineer in Powerchip Technology Corporation, Taiwan.

Dr. **Chin-Tien Yang** is currently a Senior Researcher in the Material and Chemical Research Laboratories at Industrial Technology Research Institute, Hsinchu, Taiwan. He was a Research Director and Research Manager in the Nanotechnology Research Center as well as a Project Deputy Manager and the Senior Engineer in the Electronics and Optoelectronics Research Laboratories at Industrial Technology Research Institute. He received his bachelor's degree from National Taiwan University in Taipei (Taiwan) in 1998. After receiving a bachelor's degree from National Taiwan University in 1998, he obtained his Ph.D. degree in Materials Science and Engineering from National Taiwan University in 2003. Dr. Yang's research areas include the development of opto-mechatronics systems and related materials, semiconductor equipments and their related components, wearable electronics for living aids, nanolithography apparatus and their processes.



stage or a micro-mirror that can deflect lights to any  $x$  and  $y$  positions in order to modulate the light patterns. A commercially-available projector integrates a light source, light modulator, and user interface into one system. A light source for the projector such as a laser, LED, halogen lamp, or mercury-vapor lamp, can be easily acquired, and the user only needs to connect the projector to a laptop computer with the appropriate software. An objective lens is needed to collect and collimate the projector's light to illuminate the OET chip. This study uses a commercially available LCD projector with a halogen lamp (PLC-XU350, Sanyo, Japan) as the light source.

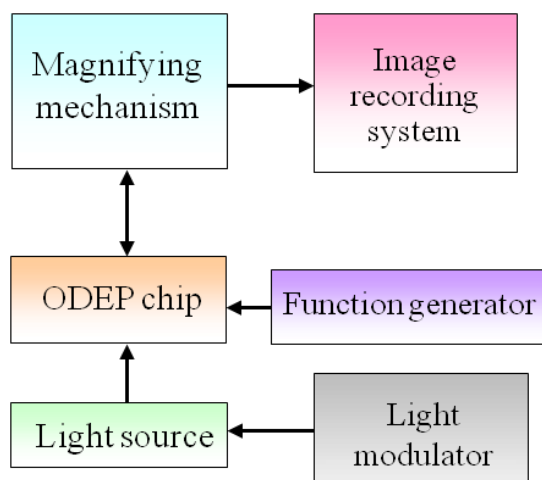


Figure 2. Schematic block diagram of the OET platform set-up.

As shown in Fig. 3, an objective lens (50 $\times$  CFI LU Plan ELWD, Nikon, Japan) is mounted on the projector head. The alignment of the light path and the objective lens should be fine-tuned; otherwise, some unwanted optical images will appear on the OET chip. Note that the distance between the objective lens and the projector head lens should be very small, allowing for the collection of a larger light area. Objective lenses with different degrees of magnification can be used for different applications. A high magnification results in a high optical image resolution, allowing for the realization of fine optical features and a high illumination power intensity. However, the field of view, which bounds the area over which such a high-magnification system can manipulate microparticles, is consequently small. A lower magnification level would allow for a larger field of view. Some other options for integrated light systems are LCD panels and organic LED panels. However, the light intensity of an LCD or organic LED panel is relatively low.

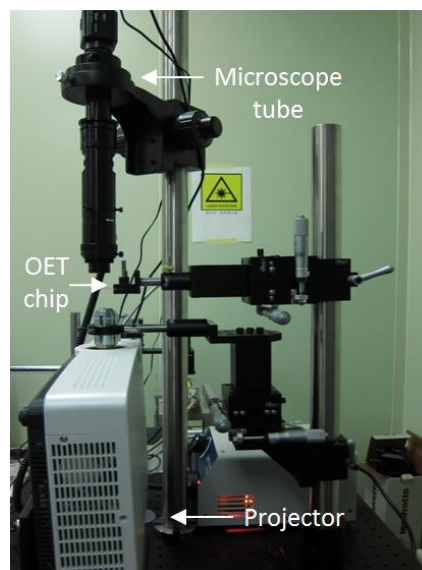


Figure 3. Photograph of the entire set-up of the OET platform. The light was projected upward and collimated through an objective lens. Experimental images were magnified by a microscope tube and recorded through a CCD camera.

The observation system can be implemented using a magnifying microscope tube or a commercial microscope. The advantage of using a commercial microscope is the ease of integration with a fluorescent module, which is useful for cell studies. A charge-coupled device (CCD) can be mounted on a microscope to record experimental images. This study uses a microscope tube (Zoom 125C, OPTEM, USA) with a 1/2" CCD (STC-620PMT, SENTECH, Japan). Two  $x$ - $y$ - $z$  stages are used to respectively control the positions of the objective lens and the OET chip (as shown in Fig. 3). The OET chip should be kept horizontal to ensure a uniform light-intensity distribution. The OET chip is translated along the  $z$ -axis to position the chip at the focal point of the light source.

#### *Fabrication of the OET photoconductive chip*

Several kinds of photoconductive materials and devices have been demonstrated to serve as the OET chip substrate including amorphous silicon [18], polymer P3HT/PCBM [19], TiOPc [20], and phototransistors [21]. Among these, thin-film amorphous silicon is one of the most commonly used photoconductive materials for OET chips because of its high stability, durability, and low mass-production cost. A phototransistor-based OET chip has been used for particle manipulation in a highly conductive medium, such as a cell-culture medium or physiological buffer solutions [21]. Such a chip shows better particle-manipulation ability than one based on amorphous silicon. However, the fabrication process of the phototransistor-based photoconductive layer is relatively complex compared to the deposition of a thin

film of amorphous silicon on the substrate. Polymers such as P3HT/PCBM or TiOPc allow for easy fabrication of the photoconductive layer but results in reduced impermeability to water as compared to non-organic materials. Therefore, in this study, amorphous silicon is used as the photoconductive material. The fabrication process of the photoconductive bottom layer is as follows. First, ITO substrates (RITEK Corp.,  $15 \Omega/\square$ ) were cleaned three times using acetone and isopropyl. Then,  $100 \text{ \AA}$  of molybdenum (Mo) was sputtered onto the ITO glass, followed by the deposition of  $1 \mu\text{m}$  of amorphous silicon using a plasma-enhanced chemical vapor deposition (PECVD) system. Note  $1 \mu\text{m}$  is a relative thick film so residual stress in the amorphous silicon should be avoided. For the continuous separation of microparticles of different sizes, a microchannel was fabricated with negative-tone photoresist, SU-8 (SU-8-50, MicroChem, Newton, MA, USA) in the OET chip. The SU-8 structures were fabricated on the ITO substrate using the standard photolithography process [15] with a thickness of  $50 \mu\text{m}$ . The ITO substrate with SU-8 microstructures was then bonded with the photoconductive layer using epoxy glue. A Teflon tube was connected to the top ITO glass layer with a drilled hole using epoxy glue to allow for the injection of fluid.

## Experimental results

### Optical patterns in the OET platform

After the platform was set up and the optical path was fine-tuned, the optical patterns projected on the OET substrate were observed through the CCD images shown in Fig. 4. The procedures for focusing the light patterns are as follows. First, the focal point of the microscope tube was adjusted to allow the light patterns to be clearly projected through the projector and objective lens. During this procedure, the position of the projector and the objective lens were fine-tuned to produce an image formed from collimated light. Then, the OET chip, which was connected to a function generator (33210A, Agilent, USA), was clipped to the sample  $x$ - $y$ - $z$  stage, and the chip was placed in the optical path of the projected light. Afterward, the position of the OET chip along the  $z$ -axis was fine-tuned to match the positions of the focal points of the projected light and of the microscope tube so the optical images and the substance in the OET chip could be clearly observed at the same time. Figure 4(a) shows that a circular field of view with a diameter of  $1.4 \text{ mm}$  can be achieved using a  $50\times$  objective lens. As described in section 2.2, a larger field of view could be achieved using an objective lens with a lower magnification. However, the resolution of

the light pattern and the intensity of the illumination were consequently decreased. Hence, the choice of magnification involves a compromise and should be made on an application-by-application basis. Figure 4(b) shows the thinnest line of light ( $\sim 10 \mu\text{m}$ ) that could be clearly projected on the OET chip. Moving optical line patterns can be used to collect nanowires suspended in the solution. With the aid of computer software, the light patterns can be easily changed, as shown in Figs. 4(c) and (d). The circular light patterns can be used to control the positions of cells or form a specific pattern of cells. Note that even when the projector is set to render the background of such patterns as “black,” some light leakages were still observed in the backgrounds of the optical patterns. Therefore, a projector with a high contrast ratio is recommended for the OET set-up (in this study, the projector contrast ratio was 500:1). We believe that the highest light/dark contrast ratio can be attained with a laser-based projector. However, the light intensity of this kind of projector is too small to smoothly manipulate particles suspended in a solution at present.

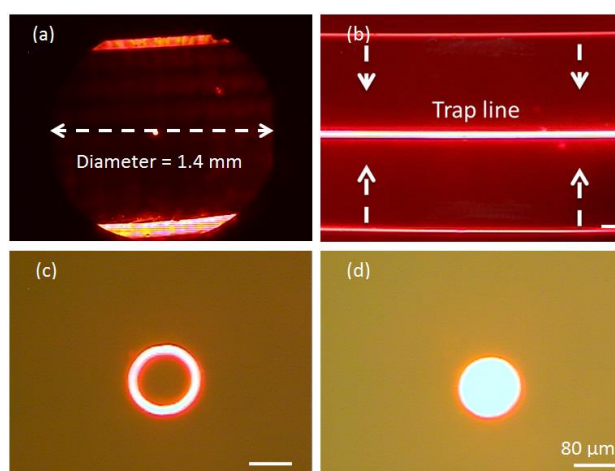


Figure 4. Optical patterns created with the OET platform. (a) Field of view of the OET system. The field of view, which bounded the area over which microparticles could be manipulated, had a diameter of about  $1.4 \text{ mm}$  when using a  $50\times$  objective lens for collimation. (b) Image of the smallest line width obtained (around  $10 \mu\text{m}$ ). (c) and (d) respectively show annular and circular patterns, demonstrating that the optical patterns can be easily changed by pattern modification using a personal computer.

### Manipulation of silver nanowires

When nanowires (NWs) are injected into the OET chip and the projected light is shined on the substrate, a positive ODEP force will be induced. The ODEP force experienced by NWs can be expressed as

$$\vec{F}_{dep} = (\pi r^2 l / 6) \epsilon_m [\text{Re}(f_{cm}) \nabla E^2]$$

where  $l$  denotes the length of the NWs [22]. Figure 5

shows that the OET platform can assemble a specific NW pattern by projecting the corresponding optical image. Given that the conductivity of NWs is higher than that of the surrounding deionized (DI) water, it is expected that the NWs will be attracted to the projected light patterns. Figure 5(a) shows that the dispersed silver NWs suspended in the DI water. The silver NWs were approximately 10  $\mu\text{m}$  in length and 100 nm in diameter. The OET chip was illuminated with a light pattern shaped like the letters “CGU” with a width of about 20  $\mu\text{m}$ , as shown in Fig. 5(b); this induced an attractive ODEP force that caused particles to be collected under an applied voltage of 10 Vpp and a frequency of 100 kHz. Then, the NWs near the light pattern were gradually attracted toward the pattern, as shown in Fig. 5(c). After 1 minute, the illuminating light and applied voltage were turned off, and a pattern of NWs corresponding to the applied optical pattern and reading “CGU” was revealed to have formed, as shown in Fig. 5(d). Note that there some NWs still adhered to the surface due to electrostatic force between the substrate and the NWs. The electrostatic force cannot be easily overcome by the ODEP force.

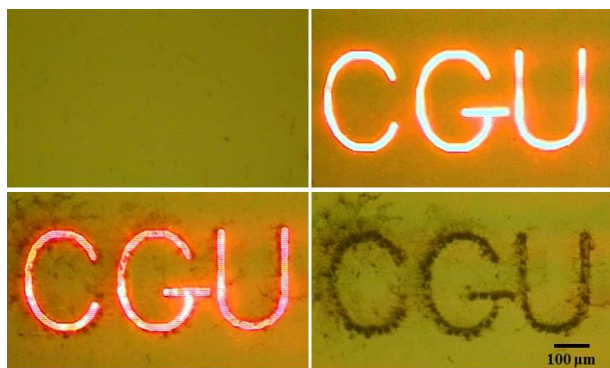


Figure 5. Series of images showing nanowire manipulation. (a) Image of nanowires suspended in a solution. (b) Illumination of the medium with a light pattern. (c) Evidence of the nanowires being attracted to the light pattern. After the light pattern is deactivated, the pattern of nanowires formed by illuminating the OET chip with a pattern of light is clearly seen in (d).

#### Continuous separation and collection of microparticles

According to Eq.(1), the strength of the ODEP force used for manipulating microparticles is proportional to the third power of the particle size. Therefore, larger particles will experience a stronger ODEP force, whereas smaller particles will experience a weaker ODEP force. In this study, we use this principle to continuously separate microparticles using a virtual electrode pattern. Figure 6 shows a sequence of photographs demonstrating the separation of smaller and larger particles into two different channels. A Y-shaped microchannel was defined by SU-8 photoresist. Then, 10- $\mu\text{m}$  and 20- $\mu\text{m}$  microparticles were initially lined up by a symmetric array of electrodes as demonstrated in our previous

study [15] (Fig. 6(a)). When the particles encounter a stationary virtual electrode tilted at an angle with respect to the paths of the particles, the larger particles are deflected by the virtual electrode, and the smaller ones pass through the virtual electrode; this separation is achieved because of the different ODEP force strengths experienced by the particles (Figs. 6(b)–(d)). Then, microparticles of two different sizes were separated and subsequently flowed into two different channels (Fig. 6(e)). Microparticles continuously flowed into the chip, passed through the focus zone, and were separated by the virtual electrode (Fig. 6(f)). Note that the flow velocity and the magnitude of the ODEP force are important factors in the continuous separation of particles. For example, a flow velocity that is too fast or an ODEP force that is too weak will be unable to alter the direction of motion of any of the microparticles. The flow velocity was set to 1  $\text{mm s}^{-1}$  through the proper configuration of the syringe pump. The ODEP force can be controlled by changing the power intensity, color, or width of the lines of the projected optical pattern [16], as well as by changing the strength or frequency of the applied electric field. In this study, a virtual electrode switch with a 15- $\mu\text{m}$  width was used to separate particles of different sizes using an applied voltage with a magnitude of 10 Vpp and a frequency of 100 kHz.

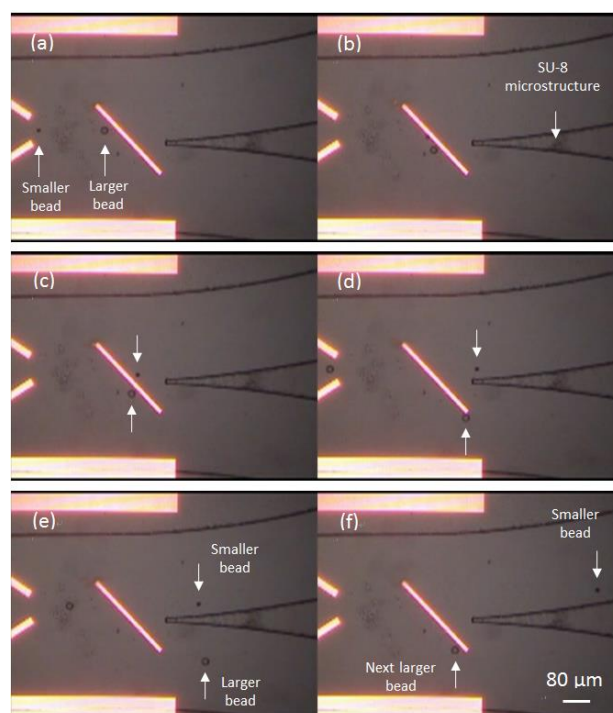


Figure 6. (a)–(f) Time sequence showing the continuous separation of microparticles by using the combination of an ODEP force and a hydrodynamic force. The smaller particles were sorted into the upper channel, while the larger ones were sorted into the lower channel.

In addition to being separated by size, microparticles can also be collected or concentrated by using a virtual electrode trap. As shown in Fig. 7,

microparticles of two sizes were first separated and then collected by the virtual electrode trap. The 10- $\mu\text{m}$  microparticles were allowed to flow into the upper microchannel and were then concentrated by a virtual electrode trap with a line width of 45  $\mu\text{m}$  (Figs. 7(a) and (b)). The 20- $\mu\text{m}$  microparticles were diverted into the lower microchannel and were then also concentrated (Figs. 7(c) and (d)). Note that ODEP forces of different magnitudes were generated in the particles' focus zone, the virtual electrode switch, and the virtual electrode trap. The largest ODEP force was generated in the virtual electrode trap to contain the microparticles. The smallest force was generated in the virtual electrode switch, which deflected larger microparticles and let the smaller microparticles pass through. The magnitude of the ODEP force was controlled by the width of the projected optical line. Note that there are some limits on the number of particles that can be captured. For 20- $\mu\text{m}$  particles, the maximum number of particles that could be collected in such a trap design was around 50. For the smaller particles, the same trap could collect more than 50 particles. This is because the larger particles would obstruct more of the microchannel, and thus the fluidic pressure upstream of the trapped particles would increase more quickly when trapping larger particles. That is why double virtual electrode traps (shown in Fig. 7) were used to collect more particles.

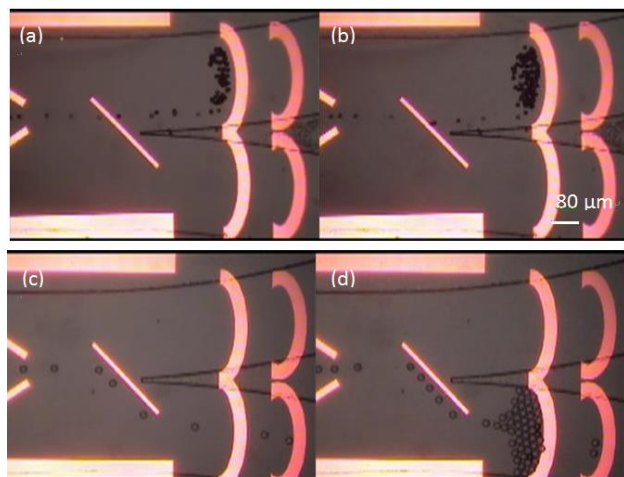


Figure 7. Separation and collection of microparticles by using a virtual electrode trap. (a) and (b) show the trapping and accumulation of smaller particles, while (c) and (d) show the same process for larger particles.

## Conclusion

An LCD-projector-based OET platform is demonstrated to achieve lines with a thickness of  $\sim 10$   $\mu\text{m}$  in the projected optical patterns. Manipulation of silver nanowires was demonstrated, allowing for the formation of specific patterns of nanowires. This technique could be extended to new types of sensors or

touch panels. In addition, microparticles with different sizes were continuously separated by combining ODEP and hydrodynamic forces. Furthermore, microparticles were collected using a trap constructed from optical images. This technique could possibly be used to enhance signals from fluorescing microparticles or dye used to stain microparticles. Various light source and magnifying mechanism options for the OET platform were discussed, and the proposed platform could potentially be used for future investigations in a variety of fields.

## Acknowledgment

The authors would like to thank the Industrial Technology Research Institute and Chang Gung University for financial support under Grant Nos. GERPD2B0021 and UERPD2B0091.

## References

- [1] E. K. Sackmann, A. L. Fulton, and D. J. Beebe, "The present and future role of microfluidics in biomedical research," *Nature*, vol. 507, pp. 181–189, 2014.  
doi: [10.1038/nature13118](https://doi.org/10.1038/nature13118)
- [1] D. Mark, S. Haeberle, G. Roth, F. von Stetten, and R. Zengerle, "Microfluidic lab-on-a-chip platforms: requirements, characteristics and applications," *Chemical Soc. Reviews*, vol. 39, no. 3, pp. 1153–1182, 2010.  
doi: [10.1039/b820557b](https://doi.org/10.1039/b820557b)
- [2] J. Nilsson, M. Evander, B. Hammarstrom, and T. Laurell, "Review of cell and particle trapping in microfluidic systems," *Analytica Chimica Acta*, vol. 649, no. 2, pp. 141–157, 2009.  
doi: [10.1016/j.aca.2009.07.017](https://doi.org/10.1016/j.aca.2009.07.017)
- [3] K. W. Oh and C. H. Ahn, "A review of microvalves," *J. Micromechanics and Microeng.*, vol. 16, no. 5, R13–R39, 2006.  
doi: [10.1088/0960-1317/16/5/R01](https://doi.org/10.1088/0960-1317/16/5/R01)
- [5] H. A. Pohl, *Dielectrophoresis*. Cambridge: Cambridge University Press, 1978.
- [6] P. Y. Chiou, A. T. Ohta, and M. C. Wu, "Massively parallel manipulation of single cells and microparticles using optical images," *Nature*, vol. 436, pp. 370–372, 2005.  
doi: [10.1038/nature03831](https://doi.org/10.1038/nature03831)
- [7] Y. H. Lin, C. M. Chang, and G. B. Lee, "Manipulation of single DNA molecules by using optically projected images," *Optics Express*, vol. 17, no. 17, pp. 15318–15329, 2009.  
doi: [10.1364/oe.17.015318](https://doi.org/10.1364/oe.17.015318)

- [8] H. Hwang, D. Han, Y. J. Oh, Y. K. Cho, K. H. Jeong, and J. K. Park, "In situ dynamic measurements of the enhanced SERS signal using an optoelectrofluidic SERS platform," *Lab on a Chip*, vol. 11, no. 15, pp. 2518–2525, 2011.  
doi: [10.1039/c1lc20277d](https://doi.org/10.1039/c1lc20277d)
- [9] W. Choi, S. H. Kim, J. Jang, and J. K. Park, "Lab-on-a-display: a new microparticle manipulation platform using a liquid crystal display (LCD)," *Microfluidics and Nanofluidics*, vol. 3, no. 2, pp. 217–225, 2007.  
doi: [10.1007/s10404-006-0124-5](https://doi.org/10.1007/s10404-006-0124-5)
- [10] A. T. Ohta, P. Y. Chiou, T. H. Han, J. C. Liao, U. Bhardwaj, E. R. B. McCabe, F. Yu, R. Sun, and M. C. Wu, "Dynamic cell and microparticle control via optoelectronic tweezers," *J. Microelectromech. Syst.*, vol. 16, no. 3, pp. 491–499, 2007.  
doi: [10.1109/jmems.2007.896717](https://doi.org/10.1109/jmems.2007.896717)
- [11] C. H. Wang, Y. H. Lee, H. T. Kuo, W. F. Liang, W. J. Li, and G. B. Lee, "Dielectrophoretically-assisted electroporation using light-activated virtual microelectrodes for multiple DNA transfection," *Lab on a Chip*, vol. 14, no. 3, pp. 592–601, 2014.  
doi: [10.1039/c3lc51102b](https://doi.org/10.1039/c3lc51102b)
- [12] Y. H. Lin and G. B. Lee, "An optically-induced cell lysis device using dielectrophoresis," *Appl. Physics Lett.*, vol. 94, no. 3, 033901, 2009.  
doi: [10.1063/1.3072593](https://doi.org/10.1063/1.3072593)
- [13] K. W. Huang, Y. C. Wu, J. A. Lee, and P. Y. Chiou, "Microfluidic integrated optoelectronic tweezers for single-cell preparation and analysis," *Lab on a Chip*, vol. 13, no. 18, pp. 3721–3727, 2013.  
doi: [10.1039/c3lc5060j](https://doi.org/10.1039/c3lc5060j)
- [14] S. B. Huang, M. H. Wu, Y. H. Lin, C. H. Hsieh, C. L. Yang, H. C. Lin, C. P. Tseng, and G. B. Lee, "High-purity and label-free isolation of circulating tumor cells (CTCs) in a microfluidic platform by using optically-induced-dielectrophoretic (ODEP) force," *Lab on a Chip*, vol. 13, no. 7, pp. 1371–1383, 2013.  
doi: [10.1039/c3lc41256c](https://doi.org/10.1039/c3lc41256c)
- [15] Y. H. Lin and G. B. Lee, "Optically induced flow cytometry for continuous microparticle counting and sorting," *Biosensors and Bioelectronics*, vol. 24, no. 4, pp. 572–578, 2008.  
doi: [10.1016/j.bios.2008.06.008](https://doi.org/10.1016/j.bios.2008.06.008)
- [16] W. Y. Lin, Y. H. Lin, and G. B. Lee, "Separation of micro-particles utilizing spatial difference of optically induced dielectrophoretic forces," *Microfluidics and Nanofluidics*, vol. 8, no. 2, pp. 217–229, 2010.  
doi: [10.1007/s10404-009-0457-y](https://doi.org/10.1007/s10404-009-0457-y)
- [17] H. Morgan, M. P. Hughes, and N. G. Green, "Separation of submicron bioparticles by dielectrophoresis," *Biophysical J.*, vol. 77, no. 1, pp. 516–525, 1999.  
doi: [10.1016/S0006-3495\(99\)76908-0](https://doi.org/10.1016/S0006-3495(99)76908-0)
- [18] P. Y. Chiou, A. T. Ohta, A. Jamshidi, H. Y. Hsu, and M. C. Wu, "Light-actuated AC electroosmosis for nanoparticle manipulation," *J. Microelectromech. Syst.*, vol. 17, no. 3, pp. 525–531, 2008.  
doi: [10.1109/jmems.2008.916342](https://doi.org/10.1109/jmems.2008.916342)
- [19] W. Wang, Y. H. Lin, R. S. Guan, T. C. Wen, and T. F. Guo, "Bulk-heterojunction polymers in optically induced dielectrophoretic devices for the manipulation of microparticles," *Optics Express*, vol. 17, no. 20, pp. 17603–17613, 2009.  
doi: [10.1364/oe.17.017603](https://doi.org/10.1364/oe.17.017603)
- [20] S. M. Yang, T. M. Yu, H. P. Huang, M. Y. Ku, L. Hsu, and C. H. Liu, "Dynamic manipulation and patterning of microparticles and cells by using TiOPc-based optoelectronic dielectrophoresis," *Optics Lett.*, vol. 35, no. 12, pp. 1959–1961, 2010.  
doi: [10.1364/ol.35.001959](https://doi.org/10.1364/ol.35.001959)
- [21] H. Y. Hsu, A. T. Ohta, P. Y. Chiou, A. Jamshidi, S. L. Neale, and M. C. Wu, "Phototransistor-based optoelectronic tweezers for dynamic cell manipulation in cell culture media," *Lab on a Chip*, vol. 10, no. 2, pp. 165–172, 2010.  
doi: [10.1039/b906593h](https://doi.org/10.1039/b906593h)
- [22] A. Jamshidi, P. J. Pauzauskie, P. J. Schuck, A. T. Ohta, P.-Y. Chiou, J. Chou, P. Yang, and M. C. Wu, "Dynamic manipulation and separation of individual semiconducting and metallic nanowires," *Nature Photonics*, vol. 2, pp. 86–89, 2008.  
doi: [10.1038/nphoton.2007.277](https://doi.org/10.1038/nphoton.2007.277)

